Ceramics-Silikáty 68 (3), 360-365 (2024)
www.ceramics-silikaty.cz doi: 10.13168/cs.2024.0035

DIFFERENTIAL THERMAL ANALYSIS OF THE CRYSTALLIZATION KINETICS IN PERLITE-BASED NANOCRYSTALLINE GLASS-CERAMICS

LYOVA GRIGORYAN*, #PETIK PETROSYAN*, LEVON ASRYAN**,
NIKOLAY KNYAZYAN***, STEPAN PETROSYAN****

** Institute of Physics, Yerevan State University,Yerevan, 0025, Republic of Armenia*
*** Department of Materials Science and Engineering, Virginia Polytechnic Institute and State University, Blacksburg, VA 24061, USA*
**** M.G. Manvelyan Institute of General and Inorganic Chemistry of the National Academy of Sciences, 0051, Republic of Armenia*
*****Institute of Radiophysics and Electronics of the National Academy of Sciences, Ashtarak, 0203, Republic of Armenia*

#E-mail: ppetros@ysu.am

Submitted February 19, 2024, accepted May 31, 2024

Keywords: Glass-ceramic material, Crystallization kinetics, Activation energy

A glass-ceramic material containing nanosized crystallites is synthesized based on the natural volcanic material perlite. Using the differential thermal analysis (DTA) method, the effect of Na_2SiF_6 (a crystallization catalyst from the fluoride group) on the glass crystallization properties is studied. The characteristic glass-transition temperature T_g, peak crystallization temperature T_p, as well as the crystallization activation energy (E_c) and Avrami index (n) are determined in terms of the catalyst content in the initial composition. A decrease in the nucleation agent content is shown to increase T_g, T_p, and E_c. The effect of the crystallization catalyst content on the crystallization mechanism and glass mechanical properties is discussed.

INTRODUCTION

The development of nanotechnology opens up broad possibilities for obtaining materials with new physical properties that can be used in various fields of engineering [1, 2]. From this point of view, of great interest are the polycrystalline glass-ceramic (GC) materials containing nanoscale crystallites. These materials, having high mechanical strength, thermal stability and high impact resistance, can be suitable for numerous applications in microelectronics, optics, medicine, and defense [3-5].

The key properties of ceramics with nanocrystalline structure (such as the mechanical strength, ballistic efficiency, dielectric permeability, and chemical stability) can be controlled by a proper selection of the materials composition and technological regimes of synthesis [6-8].

The main components of the GC materials are silica (SiO_2), aluminum oxide (Al_2O_3), sodium oxide (Na_2O), calcium oxide (CaO), and magnesium oxide (MgO) [9,10]. Based on its chemical composition, the natural volcanic material perlite [11-13] was also proposed as a feasible raw material for synthesizing the GCs.

In this work, we study the effect of the nucleation agent (Na_2SiF_6) content on the kinetics of formation and parameters of nanocrystalline perlite-based GCs.

EXPERIMENTAL

The composition of our synthesized GCs material includes: perlite (having the chemical composition of: SiO_2 – 73 %, Al_2O_3 – 13,12 %, CaO – 0,84 %, MgO – 0,24 %, Fe_2O_3 – 0,82 %, Na_2O + K_2O – 7,72 %) – 30 ÷ 70 wt. %, $CaCO_3$ - 30 ÷ 40 wt. %, Na_2CO_3 – 2 ÷ 5 wt. %. To obtain homogeneous crystallization, 3 ÷ 7 wt. % of nucleation agent Na_2SiF_6 is also added.

The GC material containing nanocrystallites was synthesized in two stages. At the first stage, the glass was melted at the temperature of 1350-1400 °C in corundum crucibles for 4-8 hours. The glass melt was then poured in preheated black iron moulds and the resulted bulks were annealed at 500-600 °C to eliminate the stress. In order to create the necessary microstructure, the samples were subjected to a two-stage heat treatment. At the first stage during which the crystal nuclei appeared and grew, the samples were kept for about an hour at the temperature of 600-700 °C. At the second stage, the temperature was elevated to 800-950 °C, and the sample was held in order to crystallize the main substance of the glass. The homogeneity of the parent glass mass and the controllability of the technological conditions of crystallizationmade it possible to obtain a non-porous GC

material with a uniform fine-grained structure and high mechanical strength.

The correct selection of the initial raw material mixture and appropriate crystallization catalyst (nucleation agent)is very important for the synthesis of the glass-crystalline material based on perlite. Research shows that their percentage significantly affects the microstructure and physical and mechanical properties of the resulting material [14].

In this work, to understand the effect of nucleating agent on the crystallization mechanism, microstructure, and properties of the GC, we study the relationship of the GC material formation kinetics with the crystallization catalyst content.

Thermal stability and crystallization kinetics were studied by the non-isothermal DTA using a Paulik-Paulik-Erdey Q-1500D derivatograph (Hungary). The calcined powder Al_2O_3 served as a reference material, the sample weight was 1 g. The phase composition of GC was identified using X-ray diffraction using a PANanlytical B.V diffractometer (Holland) (Cu-Kα radiation). The micro hardness and compressive strength of GCs samples were measured by MicroVickers Hardness Tester DV-1At-8 (China) and Ceramic Compressive Strength Testing Machine TBTTCKY-1 (China).

Determination of the kinetic parameters of nucleation and crystallization (in particular, the activation energy of crystallization and the principal crystal growth mechanisms) is important in obtaining the GCs with the desired microstructure and physical and mechanical properties.

Two types of samples were synthesized that differ only in the crystallization catalyst content in the composition of raw materials (perlite-52 wt. %, $CaCO_3$ – 38 wt. %, Na_2CO_3 – 3 wt. %). In the samples of the first (GC7) and second (GC3) series, 7 and 3 wt. % of the crystallization catalyst were added respectively.

Figure 1 shows the DTA curves for samples GC7 and GC3 for three different heating rates (α) – 5, 10, and 20 °C·min^{-1}. As can be seen from the Figure, only one exothermic peak is observed in both types of samples. Three characteristic temperatures are revealed from our DTA studies: glass transition temperature T_g, crystallization onset temperature T_c, and crystallization peak temperature T_p. The values of these characteristic temperatures for samples GC7, GC3 are given in Table 1.

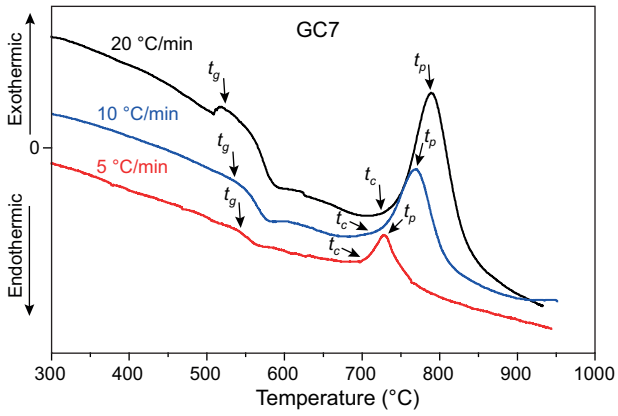

a)

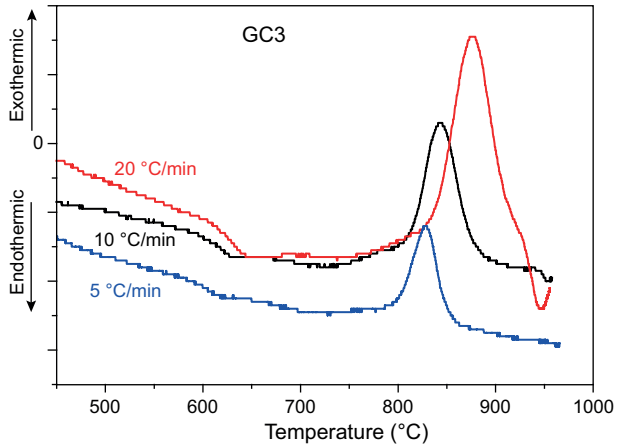

b)

Figure 1. DTA curves for samples GC7 (a) and GC3 (b) for three different heating rates (α) – 5, 10, and 20 °C·min^{-1}.

Table 1. Characteristic temperatures for samples GC7, GC3 for three different heating rates (α) – 5, 10, and 20 °C·min^{-1}.

Heating rates (°C·min^{-1})	GC7			GC3		
	T_g (°C)	T_c (°C)	T_p (°C)	T_g (°C)	T_c (°C)	T_p (°C)
5	540	697	728	569	784	829
10	556	714	769	599	753	844
20	564	722	789	617	763	876

RESULTS AND DISCUSSION

Rapid cooling of molten glass leads to the formation of a metastable supersaturated solid solution. If the glass is again subjected to heat treatment at the temperature at which the diffusion lengths of the constituent ions become comparable to inter-atomic distances in the solution, the fluctuation formation of crystal nuclei will start.

Addition of a crystallization catalyst leads to a decrease in the cohesion of the glassy framework and formation of defects that can act as crystal nucleation centers. An increase in the crystallization catalyst content, as can be seen from Table 1, leads to a decrease in T_g, which in turn is an indication of a decrease in the viscosity of the resulting glass.

Viscosity at a given temperature (T_g in our case), as is known, increases with a decrease in the fraction of broken bonds and an increase in the network packing density [15].The addition of a crystallization catalyst from the fluoride group leads to a partial replacement of oxygen with fluorine that greatly weakens the structural

network of the glass. The difference in the effect of the oxide and fluoride of the same element on the viscosity of glasses is that the introduced fluorine forms non-bridging bonds in the structure, and hence the viscous flow occurs primarily along the thermally weakened fluorine bonds in fluorine-containing glasses. This leads to a sharper decrease in the viscosity of glasses and activation energy of viscous flow. As a result of shortening of anionic silicon-oxygen groups and an increase in the number of fluoride and oxy-fluoride groups, the bond strength of glass structural groups weakens.

At a certain concentration of the introduced crystallization catalyst Na_2SiF_6, the number of weakened end-bonds of oxygen and fluorine (Si–O–Na, Si–O–Me–F) becomes sufficient to realize their structure-forming abilities and isolate the crystallization nuclei.

The higher the content of the crystallization catalyst, the higher the concentration of nuclei and the lower the viscosity of the glass, which will greatly facilitate the crystallization process.

Under the conditions of a large number of crystallization centers throughout the sample, as a result of heat treatment, nanometer-sized crystalline grains are formed that are separated by glassy layers. Using the images obtained by an atomic force microscope, the size-distribution of crystal grains was analyzed. It was shown that the crystals formed had an average size of 80-100 nm, and the size-distribution of crystals was close to log-normal [14].

Increasing the crystallization catalyst content also decreases the peak crystallization temperature. As can be seen from Table 1 above, the range of temperatures ($T_c - T_g$) that characterizes the thermal stability of the glass does not change significantly when the concentration of the catalyst is changed.

The kinetic parameters of the glass crystallization under non-isothermal conditions are determined by various models suggested by Kissinger, Matusita, Sakka and Ozawa [16-19]. In these models, it is assumed that the peak crystallization temperature depends on the heating rate α. For example, in the model proposed by Kissinger, this relationship reads as follows [16]:

$$\ln\left(\frac{\alpha}{T_p^2}\right) = -\frac{E_{ck}}{R\,T_p} + \text{const.}, \qquad (1)$$

where E_{ck} is the crystallization activation energy and R is the universal gas constant. Plotting the dependence of $\ln(\alpha/T_p^2)$ on $1/T_p$, we obtain a straight line, the slope of which will then determine E_{ck}. Figure 2 illustrates this dependence for samples with different crystallization catalyst content. The crystallization activation energy E_{ck} thus determined is176 and 289 kJ·mol^{-1} for samples GC7 and GC3, respectively. Hence the crystallization activation energy increases as the crystallization catalyst content decreases from 7 to 3 %.

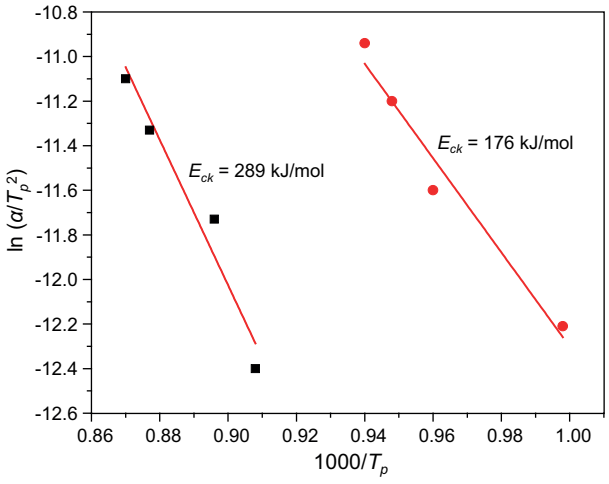

Figure 2. Dependence of $\ln(\alpha/T_p^2)$ on $1000/T_p$ (K^{-1}) for samples with different crystallization catalyst contents: GC7 (●) and GC3 (■).

Matusita and Sakka assumed that Equation 1 is valid only when the number of crystallization centers does not change during the crystal growth [17, 18]. If the crystallization centers are mainly formed during the DTA measurements, the number of which in turn varies with α, an inaccurate value for the activation energy will then be obtained using Equation 1. Hence a modified form of the Kissinger equation was proposed,

$$\ln\left(\frac{\alpha^n}{T_p^2}\right) = -\frac{m\,E_c}{R\,T_p} + \text{const.}, \qquad (2)$$

where E_c is the modified crystallization activation energy, n and m are the numerical coefficients that depend on the crystal growth mechanism. If the surface crystallization predominates, m = 1; if the bulk crystallization predominates, m = 3. The values of n and m are related. For example, n = m, if the number of the crystallization centers remains unchanged at different crystallization rates, and $m = n^{-1}$, if the crystallization occurs during the DTA and the number of the crystallization centers formed in the glass is inversely proportional to α. If the surface crystallization predominates (i.e.), then equation (3) reduces to equation (1) and E_c becomes equal to E_{ck}. In the case of bulk crystallization, E_c is not necessarily equal to E_{ck} [19, 20].

The Avrami parametercan be found from the following modified Ozawa Equation [21]:

$$\ln\left(\frac{d\,\{\ln[-\ln(1-x)]\}}{d(\ln\alpha)}\right)_T = -n, \qquad (3)$$

where x is the crystallization volume fraction at a fixed temperature for different heating rates. At a given temperature, the value of x can be defined as the ratio A_T/A, where A is the total area of the crystallization peak confined between the crystallization onset temperature T_c and temperature T_f at which the crystallization is complete, and A_T is the area confined between T_c and the current temperature.

Figure 3 shows the dependence of the crystalline fraction x on the temperature at different heating rates

for samples with different content of the crystallization catalyst. The dependence has the form of a sigmoidal curve, which indicates to the fact that the formation of the crystalline phase occurs due to combination of the nucleation and growth processes.

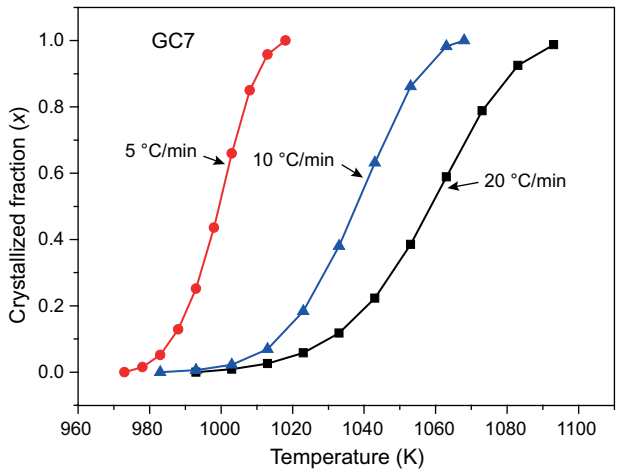

a)

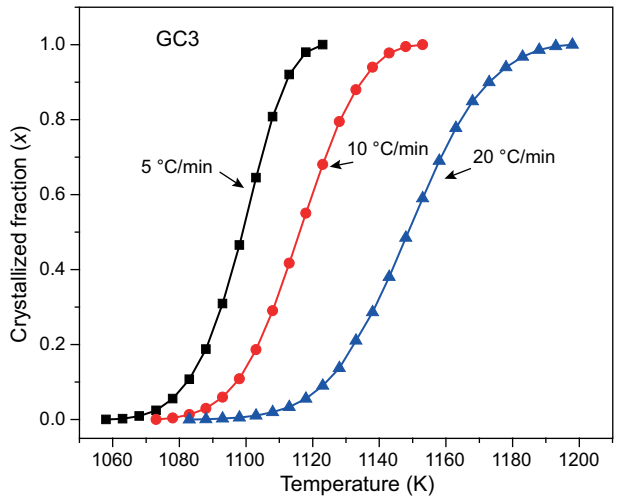

b)

Figure 3. Temperature-dependence of the crystalline fraction for samples GC7 (a) and GC3 (b) having different contents of the crystallization catalyst.

To determine the Avrami parameter n, it is necessary to plot the dependence of $\ln[-\ln(1-x)]$ on $\ln(\alpha)$ at various fixed temperatures. Figure 4 shows an example of such dependence at the temperature T = 1010K. The average values of the Avrami parameter determined from the slope of the above dependence are $n = 2.72$ and $n = 3.77$ for samples GC3 and GC7, respectively.

It can be concluded that, with the increase of the catalyst content from 3 % to 7 %, the mechanism of the glass-to-crystal transformation undergoes a significant change, namely, there occurs a transition from primarily surface nucleation and two-dimensional growth to bulk nucleation and three-dimensional growth of crystals.

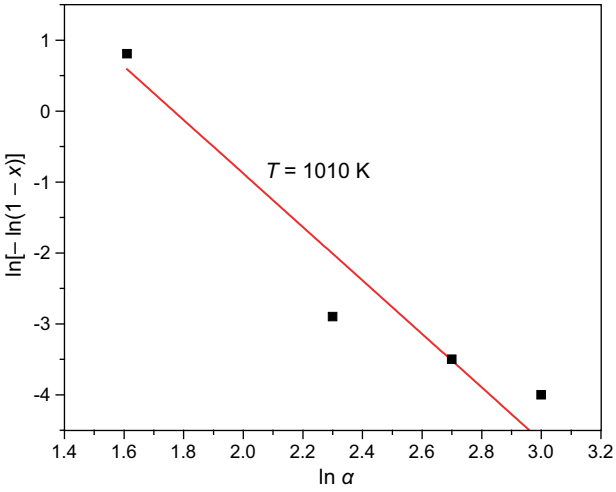

Figure 4. Dependence of $\ln[-\ln(1-x)]$ on $\ln(\alpha)$.

Based on the equation of Matusita and Sakka (2), given the values of n and m, the dependence of $\ln(\alpha^n/T_p^2)$ on $1/T_p$ was plotted. From the slop of this dependence, the crystallization activation energy E_{ck} was determined for samples GC7 and GC3 (262 and 458 kJ·mol^{-1}, respectively). The larger value of E_{ck} at 3 % catalyst is apparently also due to surface crystallization.

Another way to determine the Avrami parameter was suggested in [22], where the following relation was derived for the maximum of the crystallization rate:

$$\left(\frac{dx}{dt}\right)_p = 0.37\,\alpha\,E_{ck}\,n\,(R\,T_p^2)^{-1}\,. \qquad (4)$$

The dependence of dx/dt on the temperature is plotted in Figure 5 for different heating rates. As can be seen from the figure, $(dx/dt)_p$ increases with increasing heating rate. Having the values of $(dx/dt)_p$ at each heating rate, the corresponding values of the Avrami parameter were determined from Equation 4. Taking the average of these values as the most plausible, we found $n = 3.82$ and 2.83 for samples GC7 and GC3 respectively. These values of n are quite close to those obtained from the modified Equation 2.

Using the XRD, we examined the crystalline phase development in the glass samples. The XRD patterns for the sample GC7 are shown in Figure 6. Based on the data on the exothermic peak of the DTA, this glass-crystalline sample was obtained by first holding it for 1 h at the nucleation temperature (about 650 °C) and then for the next 2 h at the crystallization temperature (800 °C). The heating rate was 5 °C·min^{-1}. We can see the intense diffraction peaks at the angles 2ϑ = 27.4402°, 29.2035°, 30.8832, 48.3581° and 58.4470°, that correspond to reflections from the crystallographic planes (-202), (023), (212), (-334), and (027) of wollastonite ($CaSiO_3$). In addition to this major crystalline phase, this sample also clearly shows weaker diffraction lines at the angles 31.1905°, 35.2238°, 39.1596°, 44.9475°, 50.0883°, 53.0458° that are typical for the crystallographic planes

(121), (002), (112), (122), (041), and (331) of gelenite ($Al_2Ca_2SiO_7$). We can therefore conclude that perlite GCs contain wollastonite as the main crystalline phase and gelenite acting as a secondary phase.

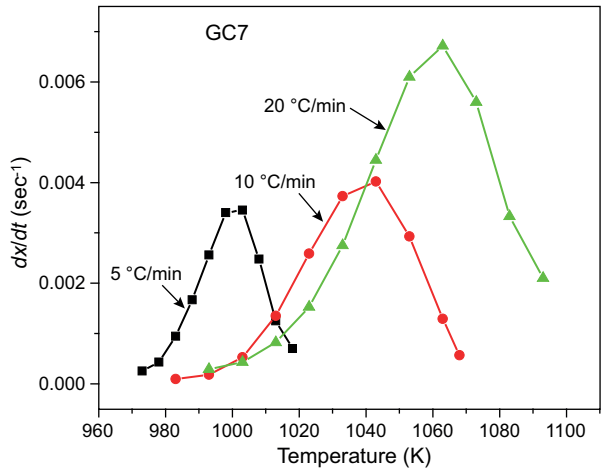

a)

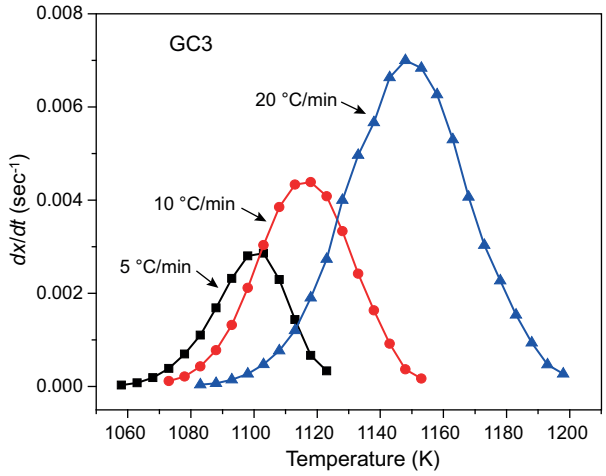

b)

Figure 5. Temperature-dependence of *dx*/*dt* at different heating ratesfor samples GC7 (a) and GC3 (b) having different contents of the crystallization catalyst.

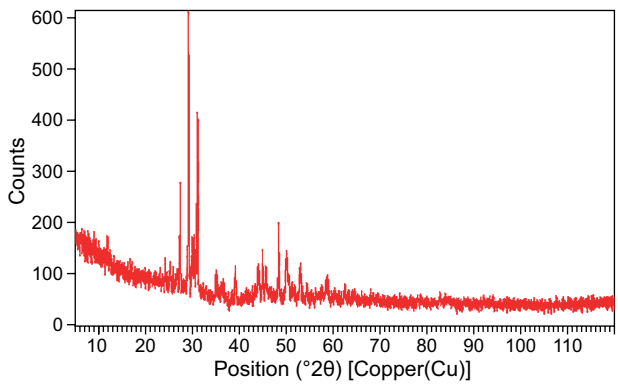

Figure 6. X-ray diffractogram (Cu-Kα) for the sample GC7 with the catalyzer content of 7 %.

As is known, the mechanical strength and hardness of a GC material having a nanocrystalline structure increase with increasing area of the nanocrystal-matrix interfaces it acts as a barrier to the movement of dislocations [23-25]. Since the concentration of nanoscale crystalline grains increases with increasing amount of crystallization catalyst, this should have a significant effect on the mechanical properties of GC.

In order to study the dependence of the compressive strength on the crystallization catalyst percentage, samples (with the sizes of 4 × 5 × 12.5 mm) were prepared that contained different fractions of the catalyst. Figure 7 shows the dependence of the compressive strength of the GC samples on the percentage of the crystallization catalyst (Na_2SiF_6). As can be seen from the Figure 7, the mechanical strength of the GCs increases from 180 to 900 MPa as the crystallization catalyst fraction increases from 3 to 7 wt. %. With the above change in the crystallization catalyst fraction, the Vickers microhardness value of the GC increases from 7 to 9 GPa [14].

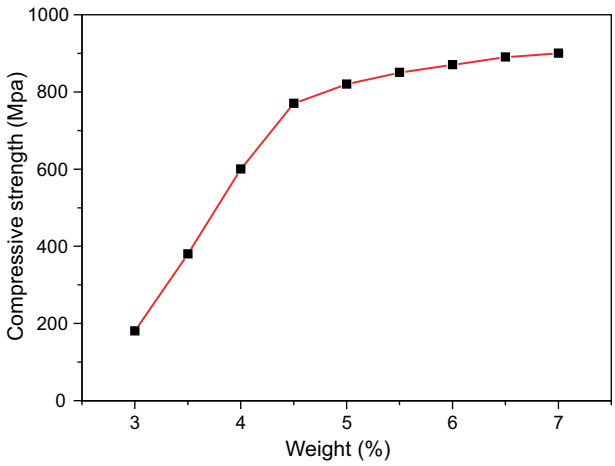

Figure 7. Compressive strength of samples against the crystallization catalyst fraction.

CONCLUSION

A glass-crystalline material containing nanoscale crystals of wollastonite and gelenite was synthesized based on the natural volcanic material perlite. Using the differential thermal analysis method, the glass crystallization properties were investigated as a function of the fraction of the crystallization catalyst (Na_2SiF_6). As the catalyst content decreases from 7 % (the samples of the first series GC7) to 3 % (the samples of the second series GC3), the crystallization activation energy increases from 176 to 289 kJ·mol^{-1} and the Avrami parameter decreases from 3.82 to 2.83. It can be therefore concluded that bulk nucleation and three-dimensional crystal growth predominate in the crystallization process in the samples of the first series, while surface crystallization predominates and two-dimensional crystallization plays

an important role in the samples of the second series. The mechanical strength of the glass ceramics increases from 180 to 900 MPa and the Vickers microhardness from 7 to 9 GPa as the crystallization catalyst fraction increases from 3 to 7 %.

REFERENCES

1. Kamakashi N. (2018). Glass-Ceramics: Properties, Applications and Technology. N.-Y.: Nova Sci. Publ.
2. Zanotto E.D. (2010): Bright future for glass-ceramics. American Ceramics Society Bulletin, 89(8), 19-27.
3. Karmakar B. (2017). Functional Glasses and Glass-ceramics: processing, properties and applications. Oxford, United Kingdom: Butterworth-Heinemann Publ.
4. Rawlings R.D, Wu J.P, Boccaccini A.R. (2006) Glass-ceramics: Their production from wastes – A Review. Journal of Materials Science, 41, 733–761.
5. Rudoi B.L. (1984). Ballistic-resistant glass-ceramic and method of preparation. US Patent No. 4 473 653.
6. Deubener J., Allix M., Davis M.J., Duran A., Höche T., Honma T. (2018): Updated definition of glass-ceramics. Journal Non-Crystalline Solids, 501, 3-10. doi: 10.1016/j.jnoncrysol.2018.01.033
7. Khater G.A., Safwat E.M., Kang J., Yue Y., Khater AGA. (2020): Some types of glass-ceramic materials and their applications. International Journal of Research, 7(3), 1-16.
8. Severenkov I.A., Ustyugova E.V., Alekseeva L.A., Zaichuk T.V., Spiridonov Y.A. (2021): Glass formation and crystallization of strontium aluminosilicate system glasses: influence of modifying additives on cooking and crystallization properties. Glass and Ceramics, 78,259–263.
9. Strnad Z. (1986). Glass-ceramic materials, Elsevier Science Publishers, Amsterdam.
10. Baik D.S., No K.S., Chun J.S. (1995): Mechanical properties of mica glass-ceramics. Journal of the American Ceramic Society,78(5), 1217-1222. doi: 10.1111/j.1151-2916.1995.tb08472.x
11. Burriesci N., Arcoraci C., Antonucci P. (1985): Physicochemical characterization of perlite of various origins. Materials Letters, 3, 103-110. doi: 10.1016/0167-577X(85)90008-4
12. http://aragatsperlite.am/eng/50/Product-specificaction
13. Yu Y., Hao X., Song Lu, Zhen L., Song L. (2016): Synthesis and characterization of single phase co-fired cordierite glass-ceramics from perlite. Journal Non-Crystalline Solids, 448, 36-42. Doi:10.1016/j.jnoncrysol, 2016. 06. 039
14. Petrosyan S.G., Grigoryan L.N., Petrosyan P.G. (2024) Perlite-based nanostructured glass-ceramics: preparation and investigation. Glass and Ceramics, 80(10), 430-435. doi: 10.1007/s10717-023-00627-0
15. Ray N.H. (1974): Composition-property relationships in inorganic oxide glasses. Journal Non-Crystalline Solids, 15, 423-434. doi: 10.1016/0022-3093(74)90148-3
16. Kissinger H. (1957): Reaction kinetics in differential thermal analysis. Analytical Chemistry, 29, 1702-1706.
17. Matusita K., Sakka S. (1979): Study on crystallization kinetics in glass by differential thermal analysis. Thermochimica Acta, 33, 351–354. doi: 10.1016/0040-6031(79)87061-6
18. Matusita K., Sakka S. (1980): Kinetic-study on crystallization of glass by differential thermal analysis-Criterion on application of Kissinger plot. Journal Non-Crystalline Solids, 39, 741–746. doi: 10.1016/0022-3093(80)90525-6
19. Mahadevan S., Giridhar A., Sing A.K. (1986): Calorimetric Measurements on As-Sb-Se Glasses. Journal Non-Crystalline Solids, 88, 11-34. doi: 10.1016/S0022-3093(86)80084-9
20. Cheng K. (2001): Evaluation of crystallization kinetics of glasses by non-isothermal analysis. Journal of Materials Science, 36, 1043-1048. Doi:10.1023/A:1004804730399
21. Ozawa T. (1971): Calculating the phase transformation kinetics using impedance spectroscopy for Sb_2Te_3. Polymer, 12, 150-158. doi: 10.1016/0032-3861(71)90041-3
22. Goel A., Shaaban E.R., Melo FCL, Ribeiro M.J, Ferreira JMF (2007). Non-isothermal crystallization kinetic studies on $MgO–Al_2O_3–SiO_2–TiO_2$ glass. Journal Non-Crystalline Solids, 353, 2383-2391. doi: 10.1016/j.jnoncrysol.2007.04.008
23. Hall E.O. (1951): The deformation and ageing of mild steel:III Discussion of results. Proceedings of the Physical Society. Section B, 64, 747–753. doi: 10.1088/0370-1301/64/9/303
24. Petch N.J. (1953): The cleavage strength of polycrystals. J. Iron Steel. 53, 25–28.
25. Zhang S. (2003): Recent advances of superhard nanocomposite coatings: a review. Surface and Coatings Technology, 167, 113–119. doi: 10.1016/S0257-8972(02)00903-9